

Small-angle X-ray scattering investigation of ionomer deformation: effect of neutralizing cation

Susan A. Visser* and Stuart L. Cooper†

Department of Chemical Engineering, University of Wisconsin, Madison, WI 53706, USA

(Received 28 June 1991; revised 10 January 1992; accepted 14 January 1992)

The influence of the neutralizing cation on the response of model polyurethane ionomers to uniaxial extension is investigated by small-angle X-ray scattering. Anisotropic scattering patterns are observed for ionomers neutralized with Na^+ , Sr^{2+} and Ca^{2+} upon elongation, with the precise nature of the response depending on the neutralizing cation. Scattering patterns of elongated ionomers neutralized with Ni^{2+} and Cd^{2+} display little or no anisotropy up to extension ratios of $\lambda = 5.0$ and 3.0 , respectively. A model invoking ionic aggregate spatial rearrangement within the polymer matrix and removal of ionic groups from the aggregates to the polymer matrix or to other aggregates is postulated to explain the results.

(Keywords: SAXS; neutralizing cation; polyurethane; ionomers; uniaxial extension)

INTRODUCTION

Extensive research has been devoted to understanding the structure–property relationships of ionomers, polymers containing a small fraction of ionic repeat units^{1–6}. It is generally accepted that the aggregation of ionic groups into microdomains, forming physical crosslinks, gives rise to many of the unique properties of ionomers, and extensive attention has been focused on the factors controlling the association. Ionic group placement⁷, degree of ionization⁸, polymer backbone/ ionic group compatibility⁹, pendant anion type^{10–13}, and choice of neutralizing cation^{9,14–18} have all been shown to influence the morphology and properties of ionomers. Correlations between the undeformed morphology of the ionomers and their physical properties have proved vital to understanding the role of ionic aggregation in determination of ionomer physical properties.

Although many studies have focused on the physical properties of ionomers subject to deformation, little attention has centred on the *morphological* response of ionomers to deformation. Previous work on the response of ionomer microstructure to deformation has focused primarily on evaluation of various models of ionomer morphology^{19–23}. A full understanding of the response of ionomers to deformation is critical to engineering of ionomers for particular uses, however, since most applications require the polymer to withstand deformations of many types.

For many applications, the aspect of the ionomer chemistry which can be most easily tailored to a particular application is the neutralizing cation type. Thus, of the factors which govern ionomer morphology and properties, an understanding of the role of neutralizing cation in the deformation response is likely

to be the most useful to design of ionomers for particular applications. One system in which the role of neutralizing cation has been studied extensively is the model polyurethane ionomers. These ionomers are characterized by a regular placement of ionic groups along the polymer backbone, leading to a more regular morphology than is found in random copolymer ionomers^{23–25}. Upon deformation, interpretation of morphological data may be easier if the initial morphology has a greater degree of regularity. The neutralizing cation in the model polyurethane ionomers can be varied by use of simple ion exchange techniques while all other factors controlling ionomer structure and properties are held constant. Thus, these polymers are excellent systems for examination of the morphological response of ionomers to deformation. The deformation response of the physical properties of sulphonated model polyurethane ionomers based on poly(propylene oxide) (PPO) and tolylene diisocyanate (TDI), neutralized with one of five cations (Na^+ , Sr^{2+} , Ca^{2+} , Ni^{2+} and Cd^{2+}), has been investigated¹⁷. Tensile testing results indicated a strong dependence of the deformation response on cation type. The appearance of a well-defined yield point in the stress–strain curves of ionomers neutralized with Na^+ , Sr^{2+} , Ca^{2+} and Cd^{2+} , but not ionomers neutralized with Ni^{2+} , also indicated the wide range of deformation responses covered by these five cations. Therefore, in this contribution, these five cations were used to neutralize sulphonated model polyurethane ionomers based on PPO and TDI, and the morphological response of these ionomers to uniaxial deformation was studied using small-angle X-ray scattering (SAXS).

EXPERIMENTAL

Sample preparation

The synthesis of the model polyurethane ionomers has been described previously¹⁰. The model polyurethane

* Present address: Eastman Kodak Company Research Laboratories, Rochester, NY 14650-2116, USA

† Author to whom correspondence should be addressed

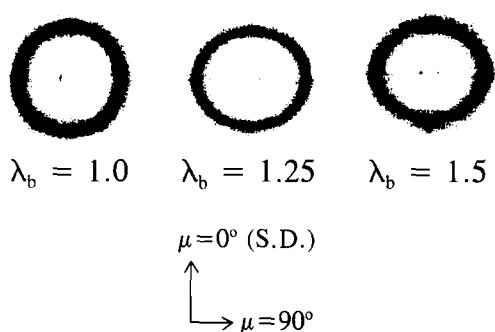


Figure 1 Two-dimensional SAXS patterns for P1SNa at various macroscopic extension ratios λ_b . S.D. indicates the stretching direction and μ is the azimuthal angle

ionomers are 1:1 copolymers of a PPO soft segment and TDI, which have sodium propyl sulphonate groups grafted solely at the urethane linkages. The molecular weight of the PPO soft segment was 1000. The sodium-neutralized ionomers were obtained directly from the grafting reaction. Ionomers neutralized with other cations were obtained by ion-exchange procedures, described previously⁹. Samples were solution-cast from *N,N*-dimethylacetamide at 60°C to form films. The films were dried in a 50°C vacuum oven for at least one week to remove residual solvent and water.

Sample nomenclature

A code was used to identify the ionomer samples: the first letter indicates the soft segment type (P = PPO); the numeral is the soft segment molecular weight in thousands; the next letter is the sulphonate pendant anion; and the final two letters are the chemical symbol for the neutralizing cation.

SAXS measurements

The SAXS data were obtained using a Rigaku Cu rotating anode point source, Charles Supper double mirror focusing optics, and a Nicolet two-dimensional detector. The scattering camera has a sample-to-detector distance of 46 cm. This configuration allowed a q ($q = (4\pi/\lambda) \sin \theta$, where 2θ is the scattering angle and λ is the wavelength of the radiation) range of 0.42 \AA^{-1} to be probed, with a minimum q of 0.015 \AA^{-1} due to the position of the beam stop. Samples were uniaxially extended to elongation ratios $\lambda_b > 1$ ($\lambda_b = L/L_0$, where L_0 is the distance between two marks on the unstretched sample and L is the distance for the stretched sample) using a stretched jig placed in the X-ray path. Samples were stretched to the desired elongation ratio and allowed to relax in the stretched configuration for at least 30 min prior to data collection. All data were collected at room temperature. The data were corrected for detector sensitivity, parasitic and background scattering (see note in text regarding some scattering patterns appearing in Figures 5, 7 and 8), and absorption of X-rays by the sample.

RESULTS AND DISCUSSION

SAXS patterns for P1SNa ionomers are shown in Figure 1. As the data show, the scattering pattern for the undeformed ionomer ($\lambda_b = 1$) is isotropic and shows only a single scattering ring. The appearance of this single

ring, or peak in a one-dimensional SAXS pattern, is generally accepted as evidence of ionic aggregation. The position of the scattering peak in q -space, denoted as q_{\max} in Table 1, closely matches previously published SAXS data for P1SNa ionomers¹⁷, as expected. The breadth of the SAXS peak, more clearly visible in Figure 2, is slightly greater than previously published results¹⁷, indicating a slightly higher degree of disorder in the sample examined here. The absence of higher order scattering peaks, which were observed in the previous study¹⁷, is another indication of the lower degree of ordering in the sample examined here.

Elongation of the P1SNa sample to $\lambda_b > 1$ results in the appearance of anisotropy in the scattering patterns, as shown in Figure 1. (Scattering results for $\lambda_b > 1.5$ could not be obtained because of uneven yielding of the sample. As previous tensile testing results¹⁷ for P1SNa ionomers identified the yield point at $\lambda_b \approx 1.4$, it is not surprising that the ionomer became highly sensitive to minute imperfections in sample preparation at elongations greater than $\lambda_b = 1.5$.) The ellipsoidal shape of the scattering patterns indicates that elliptical symmetry with respect to the azimuthal angle is present. Theoretically, this may arise from inclination of the long axes of ellipsoidal ionic aggregates towards the stretching direction or from rearrangement of isotropic ionic aggregates to an elliptically symmetrical arrangement. As the ionic aggregates may deform slightly when the sample is elongated, both mechanisms may be contributing to the observed patterns. Comparing the $\lambda_b = 1.25$ data to the $\lambda_b = 1$ data for P1SNa (see Figures 1 and 2 and Table 1), the meridional ($\mu = 0^\circ, q_{\parallel}$) scattering shifts to lower q , while the equatorial ($\mu = 90^\circ, q_{\perp}$) scattering maximum shifts to higher q values. The peak shifts are accompanied by a slight decrease in the intensity maxima of the scattering peaks. A further increase in λ_b to 1.5 has little effect on the position of the peaks in scattered intensity, but the maximum scattered intensity decreases and the breadth of the peaks increases. Also, the relative scattered intensities in the equatorial and meridional directions remain constant at a given value of λ_b , but the overall scattered intensity decreases as λ_b increases. As the intensity of the SAXS patterns is directly proportional to the electron density difference between the ionic

Table 1 Variation of peak position with extension ratio for P1S ionomers

Sample	λ_b	$q_{\parallel, \max}$	$q_{\perp, \max}$
P1SNa	1.00	0.17	0.17
P1SNa	1.25	0.15	0.18
P1SNa	1.50	0.15	0.18
P1SSr	1.00	0.17	0.17
P1SSr	1.25	0.13	0.18
P1SSr	1.50	0.13	0.19
P1SSr	2.00	0.16	0.18
P1SSr	3.00	0.14	0.19
P1SCa	1.00	0.17	0.17
P1SCa	1.25	0.14	0.19
P1SCa	1.50	0.14	0.19
P1SCa	2.00	0.15	0.19
P1SCa	3.00	0.15	0.19
P1SNI	All	0.17	0.17
P1SCd	All	0.17	0.17

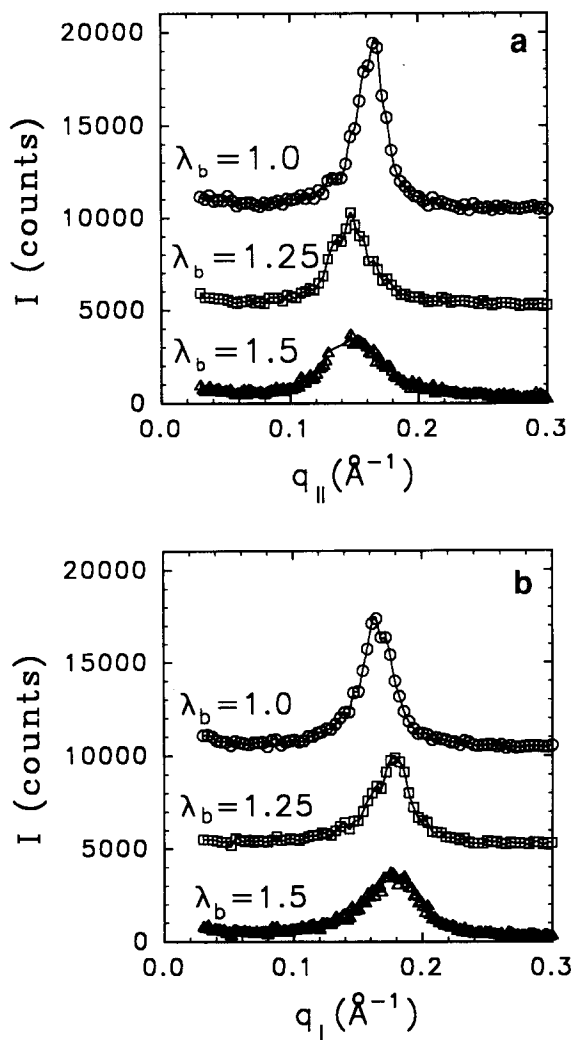


Figure 2 One-dimensional scattering patterns (a) parallel ($\mu = 0^\circ$) and (b) perpendicular ($\mu = 90^\circ$) to the stretching direction for P1SNa at various macroscopic extension ratios λ_b

aggregates and the polymer matrix, a decrease in the overall intensity as the sample is stretched suggests that the degree of phase mixing of the polymer is increasing with λ_b . Further, the breadth of the scattering peaks, as seen in *Figure 2*, increases as λ_b is increased from 1 to 1.5, also indicating that a more disordered morphology is induced by stretching.

Assuming that interparticle interference gives rise to the peak in the scattering pattern, as supported by many studies^{8,26–28}, the results for P1SNa suggest the following interpretation. As λ_b is increased from 1.0 to 1.25, the ionic aggregates are rearranged in the polymer matrix to allow a partial relaxation of the polymer chains such that the free energy of the system is minimized. As the elongation is increased to $\lambda_b = 1.5$, sufficient energy is available to begin pulling ionic groups out of the ionic aggregates, resulting in a greater number of ionic groups dispersed in the polymer matrix. Thus, the degree of phase mixing of the sample is increased while the positions of the ionic aggregates remain approximately constant.

A similar model can also be used to explain the uniaxial extension results for P1SSr, shown in *Figures 3* and *4* and summarized in *Table 1*. As with P1SNa, the scattering pattern for the undeformed sample ($\lambda_b = 1$) is isotropic and is characterized by a single peak in scattered

intensity. As λ_b is increased to 1.25, the meridional scattering peak shifts to a lower value of q , while the equatorial peak shifts to a higher q value. The extents of the shifts are somewhat greater than those observed for P1SNa. This may result from a greater cohesiveness of the ionic aggregates in P1SSr, causing the physical crosslink points to more closely follow the external deformation. In P1SNa, a less cohesive aggregate structure could result in a greater extent of ion-

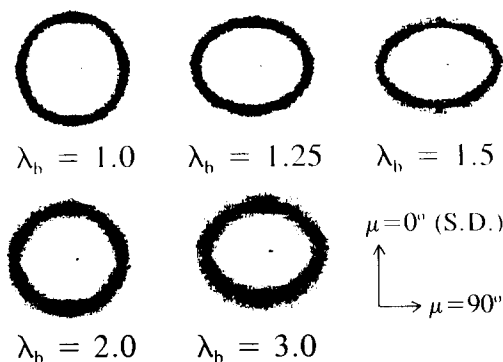


Figure 3 Two-dimensional SAXS patterns for P1SSr at various macroscopic extension ratios λ_b . S.D. indicates the stretching direction and μ is the azimuthal angle

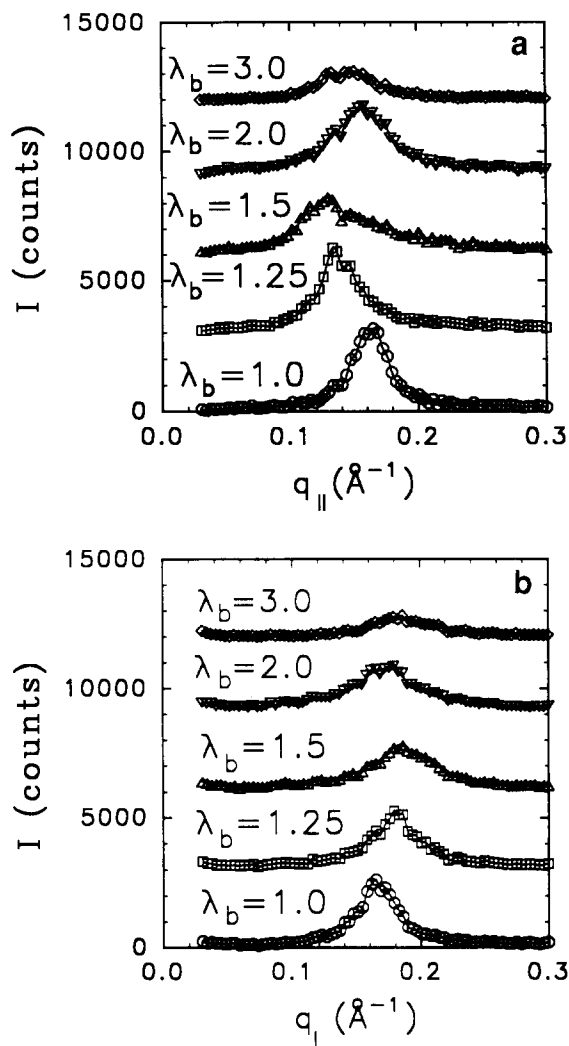


Figure 4 One-dimensional scattering patterns (a) parallel ($\mu = 0^\circ$) and (b) perpendicular ($\mu = 90^\circ$) to the stretching direction for P1SSr at various macroscopic extension ratios λ_b

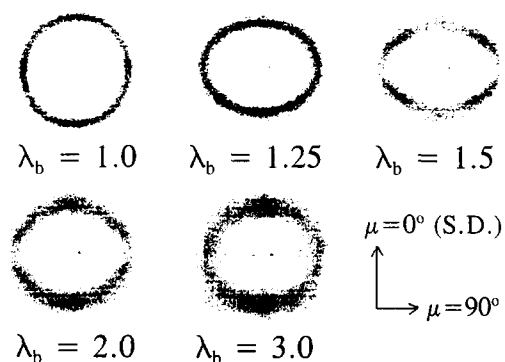


Figure 5 Two-dimensional SAXS patterns for P1SCa at various macroscopic extension ratios λ_b . S.D. indicates the stretching direction and μ is the azimuthal angle

hopping²⁹⁻³¹ (transport of ionic groups between ionic aggregates), allowing relaxation of some of the polymer chains without requiring aggregate rearrangement. This explanation is supported by previously published dynamic mechanical thermal analysis data on P1SNa and P1SSr¹⁷; these data indicated that the crosslinking efficiency of the ionic aggregates in P1SSr was greater than that of P1SNa.

Unlike P1SNa, the shift in peak position for P1SSr continues as λ_b is increased to 1.5, although the extent of the shift is less than that observed in going from $\lambda_b = 1$ to $\lambda_b = 1.25$ in P1SSr. The decreasing intensity as λ_b increases from 1.25 to 1.5 indicates that the morphology is becoming more disordered as a result of mixing of the non-ionic and ionic phases. As λ_b is increased to 2.0, there appears to be a relaxation of the ionomer; the eccentricity of the ellipsoidal scattering pattern for $\lambda_b = 2.0$ is less than that for $\lambda_b = 1.5$. Knowledge of the yield point for P1SSr can again explain these results. Tensile testing¹⁷ indicates the yield point for this ionomer is at $\lambda_b \approx 1.6$ so that yielding of the ionic aggregates may allow relaxation of the aggregate positions and consequent apparent relaxation of the SAXS pattern. The relaxation is incomplete, however, as the peak positions remain shifted to lower q for $\mu = 0^\circ$ or to higher q for $\mu = 90^\circ$ compared to the data for the undeformed ionomer ($\lambda_b = 1$). As λ_b is increased further to 3.0, the peaks shift further, indicating that aggregate position is following the macroscopic deformation, while the scattered intensity is decreasing, suggesting that simultaneous removal of ionic groups from the aggregates is occurring. A morphological rearrangement in the direction perpendicular to the stretching direction of unknown origin is suggested by the greater intensity of scattering in the meridional than the equatorial direction for the higher elongations ($\lambda_b = 2.0$ and 3.0). If the ionic aggregates are slightly non-spherical in shape, as is likely, reorientation of the aggregates may account for this feature.

A slightly different response to elongation is seen in *Figures 5 and 6* for P1SCa. Again, the undeformed sample gives an isotropic scattering pattern characterized by a single, relatively broad scattering peak. (In some scattering patterns shown in *Figures 5, 7 and 8*, the scattered intensity appears to peak at 0° , $\pm 90^\circ$ and 180° . The increased intensities in these areas are artifactual; the $0-90^\circ$ patterns result from imperfect background subtraction.) As the sample is extended to $\lambda_b = 1.25$, the meridional scattering ($\mu = 0^\circ$) peak shifts to

lower q , and the equatorial scattering ($\mu = 90^\circ$) peak shifts to higher q values. The extents of the peak shifts are greater than was observed for P1SNa but less than for P1SSr, emphasizing the importance of the neutralizing cation in the deformation behaviour.

Deformation behaviour unique to the Ca^{2+} cation appears as $\lambda_b = 1.5$ is reached. At this elongation, the scattering pattern appears as a four-point pattern, suggesting preferential orientation of the ionic particles inclined to the stretching direction and/or orientation of the aggregate lattice positions. The appearance of the four-point pattern is consistent with the explanation advanced above for the greater meridional scattering intensity of P1SSr at $\lambda_b = 2.0$ and 3.0. Orientation of anisotropic ionic particles inclined to the stretching direction, combined with the ordering of the aggregate positions, could give the four-point pattern seen for P1SCa. The appearance of this four-point pattern only for P1SCa correlates with the higher Young's modulus

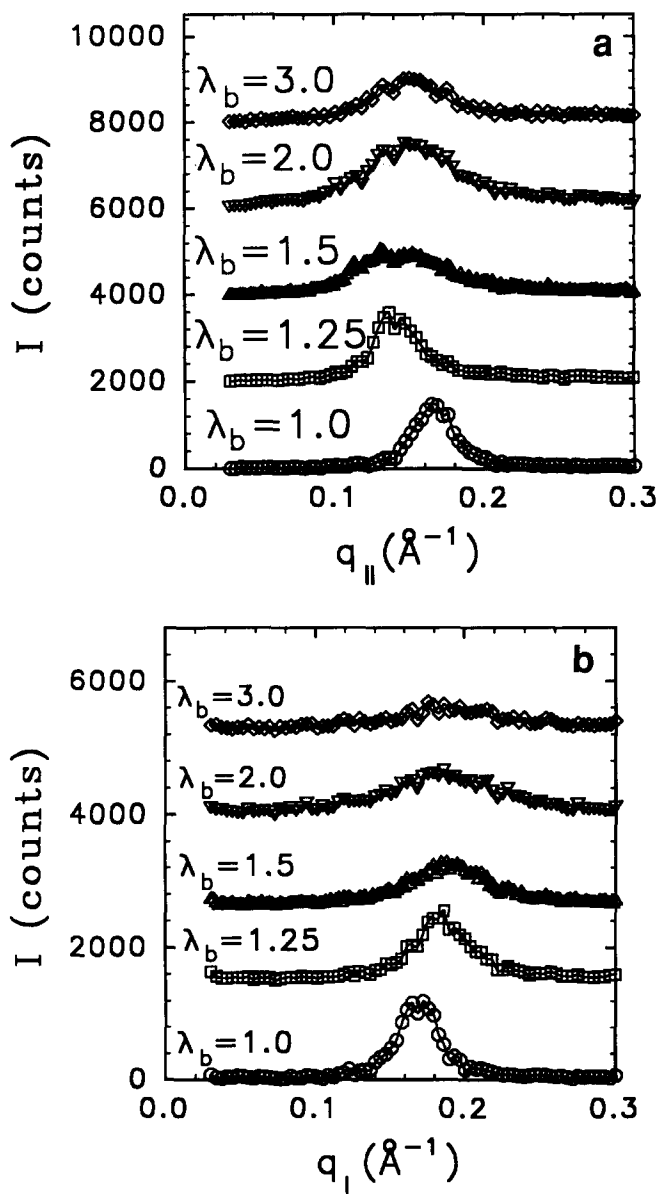


Figure 6 One-dimensional scattering patterns (a) parallel ($\mu = 0^\circ$) and (b) perpendicular ($\mu = 90^\circ$) to the stretching direction for P1SCa at various macroscopic extension ratios λ_b . Note the difference in scales between parts (a) and (b)

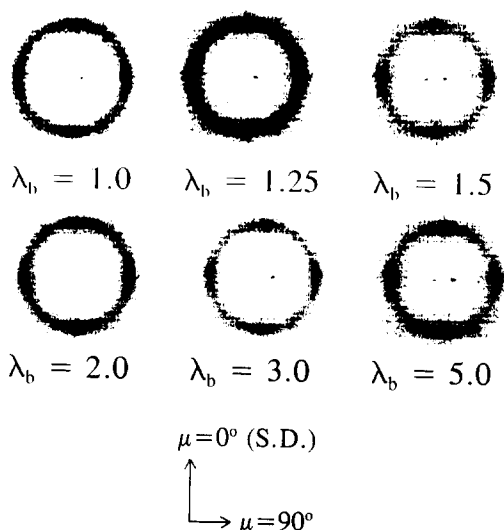


Figure 7 Two-dimensional SAXS patterns for PISNi at various macroscopic extension ratios λ_b . S.D. indicates the stretching direction and μ is the azimuthal angle

of PISCa (47.4 MPa) compared to PISsr (36.6 MPa) and PISNa (26.1 MPa)¹⁷. An ion-hopping mechanism explains these results. Ion-hopping is more difficult in PISCa so that relaxation of the polyol chains is restricted, resulting in a stiffer ionomer and one whose internal morphology more strongly resists macroscopic deformation.

As elongations of $\lambda_b = 2$ and 3 are reached for PISCa, the four-point pattern disappears. Again, yielding of the ionic aggregates probably accounts for the apparent relaxation of the morphology at $\lambda_b = 2.0$, as evidenced by the shift of the meridional and equatorial scattering peaks back towards the positions seen for $\lambda_b = 1.0$. (The yield point for this ionomer has been reported¹⁷ as $\lambda_b \approx 1.6$.) The scattered intensity also varies less with azimuthal angle μ for $\lambda_b = 2.0$ than for $\lambda_b = 1.5$, indicating a less oriented morphology. There is little change in the scattering pattern as λ_b is increased from 2.0 to 3.0. The scattered intensity decreases slightly, indicating an increase in degree of phase mixing and supporting the deformation model introduced for PISNa.

The influence of neutralizing cation on the deformation behaviour of the model polyurethane ionomers is starkly illustrated by the results for PISNi, shown in *Figure 7*. As the data show, there is some slight evidence for orientation at $\lambda_b \geq 1.5$ with the appearance of an ill-defined four-point scattering pattern. However, the scattering pattern remains predominantly isotropic in nature up to $\lambda_b = 5.0$. This correlates well with the low Young's modulus (11.1 MPa) found for the PISNi ionomer previously¹⁷ which would indicate a greater ease of ion-hopping in this ionomer than in the three ionomers discussed above. Extensive ion-hopping would allow chain relaxation, permitting the ionic aggregate positions to remain relatively unchanged and the scattering pattern to remain relatively isotropic.

The scattering patterns for PIScd also remain isotropic upon uniaxial extension. As *Figure 8* shows, the scattering from PIScd remains isotropic up to $\lambda_b = 3.0$. Previous examination of the aggregate structure of the PIScd ionomer by extended X-ray absorption fine structure spectroscopy (EXAFS)¹⁸ revealed a highly

disordered local environment around the Cd^{2+} cation, indicating that aggregate cohesiveness in this ionomer was low. Thus, extensive ion-hopping could also explain the results presented in *Figure 8*.

A comparison of the responsiveness of the ionic aggregates to external deformation is given in *Figure 9* for the ionomers which displayed anisotropy upon deformation. λ_d is the ratio of the microscopic spacing in the stretched and unstretched states, as obtained from a simple Bragg analysis of the scattering peak positions. (It should be noted that the spacing derived from a Bragg analysis, while related to the interaggregate spacing, is not a precise measure of interaggregate distances because of the irregular (non-lattice) arrangement of the ionic aggregates.) λ_b is the macroscopic deformation ratio L/L_0 , where L_0 is the unstretched length and L is the stretched length. As the data show, the deformation is nearly affine for PISNa, PISsr and PISCa up to $\lambda_b = 1.25$, but at higher values of λ_b the deformation is highly non-affine. Until the yield point is reached, the microscopic spacings change little from the values attained at $\lambda_b = 1.25$. At elongations greater than the yield points, relaxation of the spacings towards their

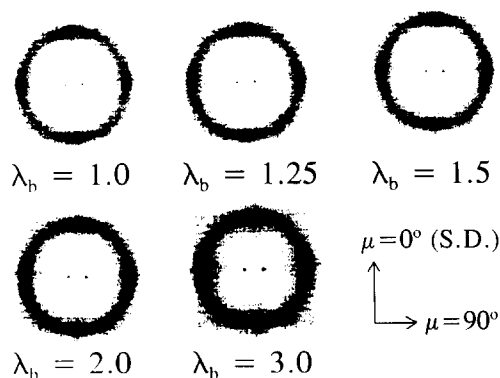


Figure 8 Two-dimensional SAXS patterns for PIScd at various macroscopic extension ratios λ_b . S.D. indicates the stretching direction and μ is the azimuthal angle

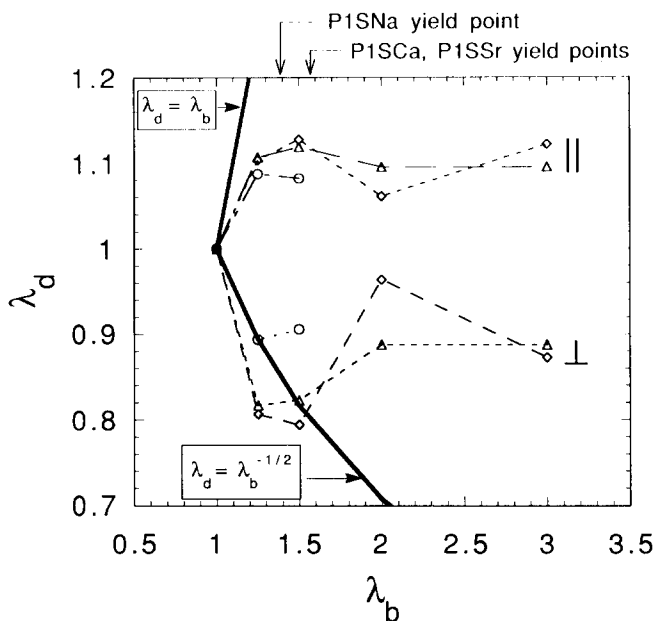


Figure 9 Comparison of the microscopic (λ_d) and macroscopic (λ_b) extension ratios for PISNa (○), PISCa (△) and PISsr (◇). Bold lines indicate the affine deformation predictions

unstretched values are seen for P1SCa and P1SSr, with gradual increases of the spacings again seen for yet higher elongations. The responsiveness of the ionic aggregate spacings to external deformation is clearly illustrated in this figure, with P1SNa showing the smallest response (of the ionomers displaying anisotropy) and therefore, presumably the greatest extent of hopping of ionic groups between aggregates or to the polymer matrix, followed by P1SSr and then closely by P1SCa.

CONCLUSIONS

The morphological response of sulphonated model polyurethane ionomers neutralized with Na⁺, Sr²⁺, Ca²⁺, Ni²⁺ or Cd²⁺ to uniaxial extension was examined using SAXS. The P1SNa, P1SSr and P1SCa ionomers exhibited anisotropic scattering patterns upon slight extension to $\lambda_b = 1.25$, and the extent of the shift in microscopic spacing at this elongation was seen to follow the predictions of affine deformation. At higher elongations, deformation for P1SNa, P1SSr and P1SCa was highly non-affine, with microscopic spacings varying less than would be predicted by an affine deformation model. Scattered intensities decreased with increasing λ_b , indicating an increasing degree of phase mixing as the samples were stretched. Yielding of the ionic aggregates was seen to strongly affect the observed morphology of the highly stretched samples, with apparent relaxation of the stretched configurations occurring at elongations greater than the yield point. A model of aggregate rearrangement at low elongations, accompanied more strongly at higher elongations by removal of ionic groups from their initial positions in the ionic aggregates to different aggregates or to the polymer matrix, was advanced to explain the results.

The deformation response of each ionomer examined was slightly different, illustrating the importance of the role of the neutralizing cation. Aggregate rearrangement in P1SNa was slightly less extensive than in P1SSr, resulting in ellipsoidal scattering patterns with slightly less eccentricity for elongated P1SNa samples. The morphological response of P1SCa was even greater, with a four-point scattering pattern appearing at the elongation closest to, yet still below, its yield point. Two ionomers examined, P1SNi and P1SCd, showed little or no anisotropy in their scattering patterns upon elongation. It was speculated that substantial ion-hopping in these ionomers allowed relaxation of the ionomer morphologies after each elongation was reached. A correlation was observed between ionomers where ion-hopping was suggested to proceed with greater ease and ionomers in which low tensile moduli had been found previously. Thus, the results of this work underline the critical importance of aggregate cohesiveness and cation chemistry in determining the response of ionomers to deformation.

ACKNOWLEDGEMENTS

Special thanks go to Professor R. E. Cohen and Dr Kostas Douzinas for their assistance in collection of the

small-angle X-ray scattering data presented in this paper. Support for this work was provided by the US Department of Energy through grant DE-FG02-88ER45370, and by the donors of the Petroleum Research Fund, administered by the American Chemical Society, through grant 20343-AC7. S.A.V. gratefully acknowledges the fellowship support of the American Association of University Women Educational Fund in the form of an Engineering Dissertation Fellowship.

REFERENCES

- Eisenberg, A. and King, M. 'Ion Containing Polymers: Physical Properties and Structure', Academic Press, New York, 1977
- MacKnight, W. J. and Earnest, T. *Macromol. Sci. Rev. Macromol. Chem.* 1981, **16**, 41
- Eisenberg, A. and Bailey, F. (Eds) 'Coulombic Interactions in Macromolecular Systems', ACS Symposium Series 302, American Chemical Society, Washington, DC, 1986
- Tant, M. and Wilkes, G. J. *Macromol. Sci., Rev.* 1988, **C28**, 1
- Lantman, C. W., MacKnight, W. J. and Lundberg, R. D. *Annu. Rev. Mater. Sci.* 1989, **19**, 295
- Fitzgerald, J. J. and Weiss, R. A. *J. Macromol. Sci., Rev.* 1988, **C28**, 99
- Brockman, N. L. and Eisenberg, A. *J. Polym. Sci.: Polym. Phys. Edn* 1985, **23**, 1145
- Yarusso, D. J. and Cooper, S. L. *Macromolecules* 1983, **16**, 1871
- Ding, Y. S., Register, R. A., Yang, C.-Z. and Cooper, S. L. *Polymer* 1989, **30**, 1204
- Visser, S. A. and Cooper, S. L. *Macromolecules* 1991, **24**, 2576
- Visser, S. A. and Cooper, S. L. *Macromolecules* 1991, **24**, 2584
- Hashimoto, T., Fujimura, M. and Kawai, H. in 'Perfluorinated Ionomer Membranes' (Eds A. Eisenberg and H. L. Yeager), ACS Symposium Series 180, American Chemical Society, Washington, DC, 1982, p. 217
- Lundberg, R. D. and Makowski, H. S. in 'Ions in Polymers' (Ed. A. Eisenberg), ACS Symposium Series 187, American Chemical Society, Washington, DC, 1980
- Register, R. A., Foucart, M., Jerome, R., Ding, Y. S. and Cooper, S. L. *Macromolecules* 1988, **21**, 1009
- Broze, B., Jerome, R., Teyssie, Ph. and Marco, C. *Macromolecules* 1983, **16**, 996
- Yarusso, D. J., Ding, Y. S., Pan, H. K. and Cooper, S. L. *J. Polym. Sci., Polym. Phys. Edn* 1984, **22**, 2073
- Visser, S. A. and Cooper, S. L. *Polymer* 1992, **33**, 920
- Visser, S. A. and Cooper, S. L. *Polymer* 1992, **33**, 930
- Fujimara, M., Hashimoto, T. and Kawai, H. *Macromolecules* 1981, **14**, 1309
- Fujimara, M., Hashimoto, T. and Kawai, H. *Macromolecules* 1982, **15**, 136
- Visser, S. A. and Cooper, S. L. *Macromolecules* 1992, **25**, 2230
- Dreyfus, B., Gebel, G., Aldebert, P., Pineri, M., Escoubes, M. and Thomas, M. *J. Phys. France* 1990, **51**, 1341
- Roche, E. J., Stein, R. S., Russell, T. P. and MacKnight, W. J. *J. Polym. Sci., Polym. Phys. Edn* 1980, **18**, 1497
- Ding, Y. S., Register, R. A., Yang, C.-Z. and Cooper, S. L. *Polymer* 1989, **30**, 1213
- Eisenberg, A., Hird, B. and Moore, R. B. *Macromolecules* 1990, **23**, 4098
- Williams, C. E., Russell, T. P., Jerome, R. and Horrión, J. *Macromolecules* 1986, **19**, 2877
- Register, R. A., Pruckmayr, G. and Cooper, S. L. *Macromolecules* 1990, **23**, 3023
- Yarusso, D. J. and Cooper, S. L. *Polymer* 1985, **26**, 371
- Ward, T. C. and Tobolsky, A. V. *J. Appl. Polym. Sci.* 1967, **11**, 2903
- Sakamoto, K., MacKnight, W. J. and Porter, R. S. *J. Polym. Sci. A-2* 1970, **8**, 277
- Hara, M., Eisenberg, A., Storey, R. F. and Kennedy, J. P. in 'Coulombic Interactions in Macromolecular Systems' (Eds A. Eisenberg and F. Bailey), ACS Symposium Series 302, American Chemical Society, Washington, DC, 1986, p. 302